On a pulsating jet from the end of a tube, with application to the propulsion of certain aquatic animals

By J. SIEKMANN

College of Engineering, University of Florida, Gainesville, Florida, and U.S. Naval Ordnance Test Station, China Lake, California

(Received 13 April 1962 and in revised form 29 October 1962)

The present paper discusses the hydrodynamics and propulsive properties when a jet of fluid is ejected from the opening of a tube. Formulas for the calculation of the thrust are provided and the basic equations for the horizontal rectilinear motion of a rigid torpedo-like body are studied in some detail. The results may be applied to investigate in an elementary way the locomotion of certain aquatic animals.

1. Introduction

The question of how nature has solved the problem of forward drive in living creatures in water is indeed an interesting and challenging one and it is the purpose of this analysis to pursue the thrust generation and locomotion of certain marine animals belonging to the class of cephalopods, particularly squids, octopuses and cuttlefish. These animals, just as jelly fish and salps, swim by jet-propulsion. From the literature we will quote a remark by Prandtl (1952, pp. 237–238), and the following two references. In his book Haley (1958), makes the following statement: 'As with most of man's technical achievement, a point of origin for reactive propulsion may be found in nature. Here the squid (loligo, a mollusk) propels itself by syphoning and ejecting water,....'

The other quotation is found in the fascinating book by Lane (1960, Ch. 4):

'Ages before men discovered jet-propulsion, cephalopods were jetting through primeval seas. Some of the smaller species of squid are the best examples of these natural jets, their swift movements earning them such names as sea arrow and flying squid (*Onychoteuthis*, etc.). The propulsive force is sea water, shot in fast repeated pulses from a single nozzle, called the funnel or siphon, on the ventral or under side of the body.

'Water enters round the free edge, or collar, of the mantle at the "neck". It is drawn by expansion of the mantle walls into the mantle cavity which acts as a compression chamber. During the intake of water, the funnel is partially collapsed and closed. Then the inlet is sealed in three ways. Cartilaginous ridges on the inside of the mantle lock into corresponding depressions on the sides of the funnel; the head is retracted towards the body (visceral mass); and valve-like extensions of the sides of the funnel seal the rest of the opening. The heavily muscled walls of the mantle cavity contract violently, and the water is driven at high speed through the muscular funnel which protrudes through the inlet. It is the pressure of this escaping water which distends the side valves of the funnel. A muscular valve inside the external opening

of the funnel controls the flow, and stops water entering from outside. The squid can point the funnel forwards or backwards, and as the jet of water shoots one way, the squid, by the law of action and reaction, is driven in the opposite direction.

'Although the principle of jet-propulsion is the same throughout the Cephalopoda, there are differences in the mechanism. The above description is generally true of all fast and medium-fast species of squid, but some of the slower swimmers, such as the Cranchiidae, have parts of the mantle permanently fused to the head. Octopuses have only the ventral edge free and the locking mechanism at the neck is weaker than the cartilaginous mechanism of the decapods. Octopuses have no internal funnel valve and some, such as the *Cirromorpha,* have only a very narrow opening. In other octopuses (*Chunioteuthis*) the only opening is the funnel, so that water enters and leaves the mantle cavity by the same aperture. In the nautiluses (*Nautilus*), the most primitive cephalopods, the water is drawn in and expelled by pulsations of the funnel.'

A schematic sketch of a common squid (*Loligo* species) is given in figure 1. Most squids have a fusiform, or torpedo-shaped, body, terminated either by one end or two side fins. All squids have eight arms which are of unequal length in many species and two tentacles. The body, strengthened by the internal shell, is streamlined for swift movement through water.

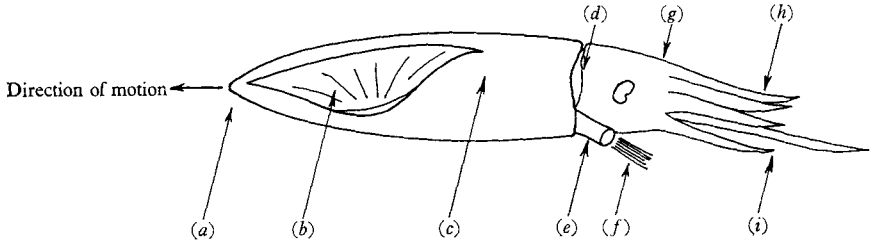

FIGURE 1. Schematic sketch of a common squid. (*a*) Back or posterior end of the body which travels first through the water; (*b*) fin; (*c*) body or 'mantle', contracts and forces water from the funnel opening; (*d*) inhalent opening (paired); (*e*) funnel; (*f*) jet-stream; (*g*) head; (*h*) arms or 'tentacles'; (*i*) front or anterior end of the animal which travels behind during the usual movement.

The excess of momentum in the flow behind the squid leads to the concept of a kind of pulsating internal-flow pump jet. Now the excess pressure inside the tube is, of course, unknown, but if there is to be an average thrust (or drag) the flow cannot be irrotational. The body must shed vorticity into the fluid. But from the existence of vortices, we can conclude that an impulsive pressure force was acting in the past and, in principle, we could determine experimentally its rate and the area it acted upon provided that other influences did not change considerably the shape of the vortices. We shall restrict our investigation to a simple model and although a complete propulsion cycle consists of a suction and an ejection, we will consider in detail the latter only.

2. The mechanism of propulsion

Let us suppose that the body of a squid is composed in essence of a hollow section joined to an intake and joined to a well rounded orifice of circular cross-section (funnel). This system will be called a 'jet propeller' (figure 2). In order to relate this simplified model to the actual situation in the squid, the obvious

differences between both are to be stressed. Differences which immediately spring to mind are:

(i) the body of the animal decreases in cross-sectional area as the jet is produced, so decreasing its drag;

(ii) the jet runs close under the head when the tube is directed 'backward' and this must affect the flow considerably—the tentacles are used to direct the flow;

(iii) the opening of the funnel changes in size as the thrust is made.

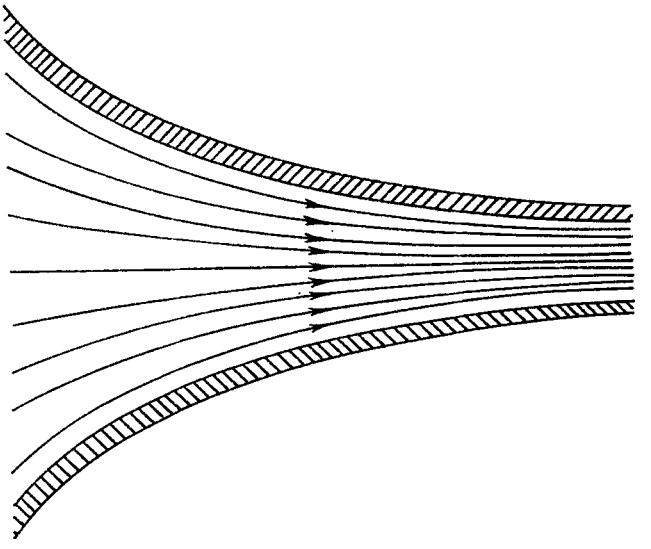

FIGURE 2. Outflow from a well-rounded orifice.

It is evident that the differences pointed out will affect the analysis considerably; however, the propulsion process taking place in the body of the animal is so complicated that a detailed theoretical investigation seems to be beyond the scope of a mathematical treatment. Thus, for a first approximation we restrict our study to the simplified approach described above.

First of all we assume that we have acting certain imposed forces, which hold the 'jet propeller' at rest with respect to a Cartesian co-ordinate system fixed in space. This infinitely extended space is completely filled with an ideal incompressible liquid, flowing with a constant velocity in the direction of the positive x-axis. As the consequence of an excessive pressure, produced in the hollow, fluid is ejected with a considerable velocity to the 'rear', i.e. in the direction of the translatory flow. During the periodic thrust intervals, we suppose that the exhaust has a uniform mean velocity over the cross-section of the discharge nozzle. At the sharp trailing edge of the orifice, vortex rings originate which travel onwards. If the efflux continues long enough, the vortex wake will extend far downstream forming a long oriented contracting jet stream with an asymptotically constant interior velocity. Such a formation preserves its grouping arrangement for a while, but has a tendency to instability and breaks up into

singular vortex lumps, without, however, any feedback to the aperture. In the following we divide our investigations into two parts: in the first one we study the so-called quasi-one-dimensional flow; in the second, a two-dimensional treatment of the flow field.†

A. *The one-dimensional theory of the unsteady periodically working jet propeller*

Let us assume that the jet propeller is immersed in a parallel flow U_0, which is constant with respect to time (figure 3). At the cross-section a–a of the jet propeller a periodically varying pressure jump $\Delta p(t)$ is generated so that the forces exerted on the fluid have the same direction as the streamlines, i.e.

$$\Delta p(t)\, A \geqslant 0, \tag{1}$$

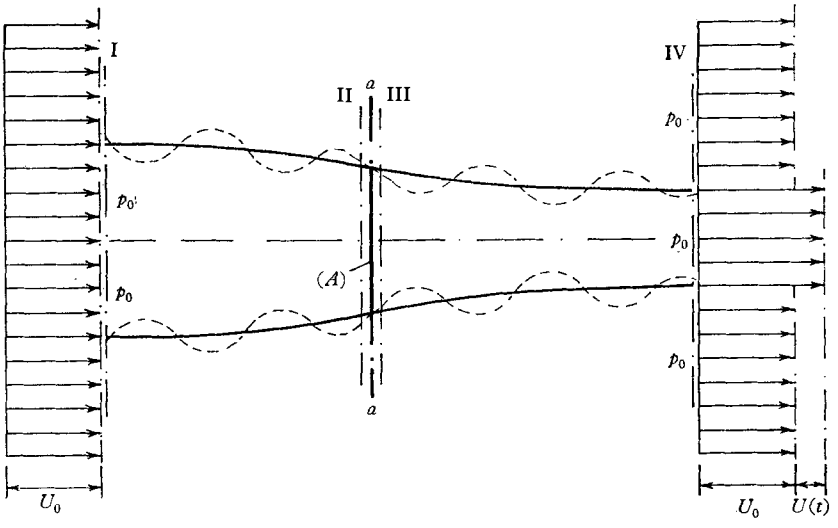

FIGURE 3. Schematic sketch of the instantaneous flow pattern of an unsteady periodically working jet propeller.

provided that the forces in the direction of flow are assumed to be positive. The pressure distribution $\Delta p(t)$ should be uniform over the area A of the surface (A) of the cross-section a–a. We denote the period of the function $\Delta p(t)$ by T_0;

$$\Delta p(t+T_0) = \Delta p(t). \tag{2}$$

At the cross-section I, which is located far upstream from the propeller, we have the undisturbed parallel flow U_0 and a constant pressure p_0.

At the location of the propeller, i.e. between the cross-sections II and III, the fluid is accelerated as a result of the pressure jump $\Delta p(t)$. The region of the fluid particles which are supposed to pass the surface (A) and the particles which are already in the wake of the propeller is indicated by the broken line.

The cross-section IV is located far downstream from the propeller. In that

† See also Dickmann (1950) and Schiele (1961).

region a pressure equilization is assumed to have occurred, so that everywhere we have again the pressure p_0. We must note, however, that this section is passed by the fluid particles of the 'slip stream' with an increased velocity $U_0 + U(t)$, where $U(t)$, the 'supervelocity' in the jet, is a periodic function of time.

In order to determine the thrust produced by the jet propeller, we apply the momentum theorem, as derived by Schiele (1961) for motions which are

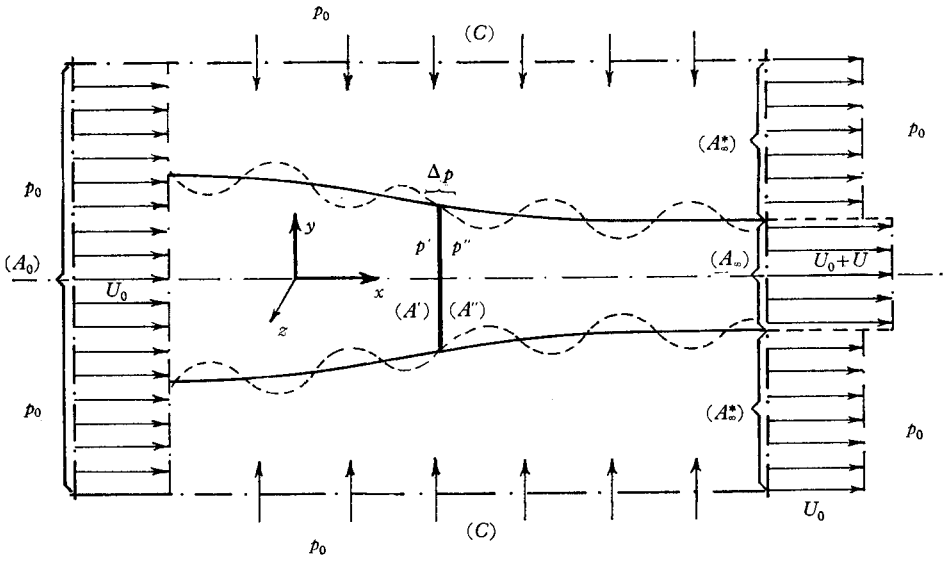

FIGURE 4. Control surface around the jet propeller.

steady with respect to average values. Disregarding body forces (such as gravity) we obtain

$$\rho T_0^{-1} \int_0^{T_0} \iint_S \mathbf{v}(\mathbf{v}.\mathbf{n})\, dS dt + T_0^{-1} \int_0^{T_0} \iint_S p\mathbf{n}\, dS dt = 0, \tag{3}$$

where $\mathbf{v} = \{u, v, w\}$ denotes the velocity vector with components in the x-, y-, z-directions, respectively, and $\mathbf{n} = \{\cos\alpha, \cos\beta, \cos\gamma\}$ the outward unit normal vector of a control surface S, whereby α, β, γ are the direction angles of the outward normal on S with the positive x-, y-, z-axes, respectively.

The control surface S enclosing the jet propeller is shown in figure 4. Due to the fact that we have an axisymmetrical problem, it is sufficient to consider the forces in the x-direction only. Hence

$$\begin{aligned}\rho T_0^{-1} \int_0^{T_0} \iint_S u(u\cos\alpha + v\cos\beta + w\cos\gamma)\, dS dt + T_0^{-1} \int_0^{T_0} \iint_S p\cos\alpha\, dS dt \\ = \rho T_0^{-1} \int_0^{T_0} \left\{ \iint_{(A_0)} + \iint_{(A_\infty^*)} + \iint_{(A_\infty)} + \iint_{(C)} + \iint_{(A')} + \iint_{(A'')} \right\} dS\, dt \\ + T_0^{-1} \int_0^{T_0} \iint_S p\cos\alpha\, dS dt = 0, \end{aligned} \tag{4}$$

where (C) indicates the lateral area of a circular cylinder whose axis coincides with the x-axis.

The contributions of the individual parts of the bounding surface yield after some straightforward calculations

$$\rho T_0^{-1} \int_0^{T_0} \iint_S u(u\cos\alpha + v\cos\beta + w\cos\gamma)\, dS\, dt$$
$$= \rho T_0^{-1} \int_0^{T_0} [U_0 U(t) + U^2(t)]\, A_\infty dt, \qquad (5)$$

where A_∞ denotes the area of the surface (A_∞). The pressure integral of equation (4) yields the value zero with regard to the exterior bounding surfaces, since (A_∞) and (A_∞^*) are located so far away from the propeller that the pressure equalization has taken place. Thus,

$$T_0^{-1} \int_0^{T_0} \iint_S p\cos\alpha\, dS\, dt = T_0^{-1} \int_0^{T_0} \iint_{(A')} p'\, dS\, dt + T_0^{-1} \int_0^{T_0} \iint_{(A'')} p''\, dS\, dt. \qquad (6)$$

Now let us suppose a uniform distribution of the pressure jump

$$\Delta p = p'' - p' \qquad (7)$$

over the surface

$$(A) = (A') = (A''); \quad (A') \uparrow (A), \quad (A'') \downarrow (A). \qquad (8)$$

Then we find from equation (6)

$$T_0^{-1} \int_0^{T_0} \iint_S p\cos\alpha\, dS\, dt = -T_0^{-1} \int_0^{T_0} \Delta p A\, dt.$$

Defining a time-average value of the thrust by

$$\bar{T} = T_0^{-1} \int_0^{T_0} \Delta p A\, dt, \qquad (9)$$

we have from equations (4), (5), (6) and (9)

$$\bar{T} = \rho T_0^{-1} U_0 \int_0^{T_0} U A_\infty dt + \rho T_0^{-1} \int_0^{T_0} U^2 A_\infty dt. \qquad (10)$$

Denoting time-average values by a bar,

$$T_0^{-1} \int_0^{T_0} U A_\infty dt = \overline{U(t)\, A_\infty(t)}, \quad T_0^{-1} \int_0^{T_0} U^2 A_\infty dt = \overline{U^2(t) A_\infty(t)},$$

we can rewrite equation (10) to yield

$$\bar{T} = \rho U_0 \overline{U(t)\, A_\infty(t)} + \rho \overline{U^2(t)\, A_\infty(t)}. \qquad (11)$$

We note that for the steady case, i.e. for constant U and A_∞ with respect to time, equation (11) is transformed into

$$T = \rho U A_\infty (U_0 + U), \qquad (12)$$

which is in agreement with the known results of the axial momentum propeller theory of Rankine–Froude.

Now we want to derive another expression for the thrust by using the Bernoulli equation (cf. Prandtl 1952, p. 39)

$$-\frac{1}{\rho}\frac{\partial p}{\partial s} + g\cos\delta = \frac{\partial}{\partial s}\left(\frac{q^2}{2}\right) + \frac{\partial q}{\partial t}. \qquad (13)$$

In this equation s denotes the co-ordinate in the direction of the streamline, g the constant gravitational acceleration, δ the angle between ds and the direction of g, and q the velocity in the direction of flow. Neglecting gravity and integrating from a position s_1 to a position s_2, we obtain

$$\frac{p_2}{\rho}-\frac{p_1}{\rho}+\frac{q_2^2}{2}-\frac{q_1^2}{2}+\int_{s_1}^{s_2}\frac{\partial q}{\partial t}ds=0, \tag{14}$$

where the indices 1 and 2 refer to the values at positions s_1 and s_2. Assuming p and q as periodic functions of time the foregoing equation yields

$$(\rho T_0)^{-1}\int_0^{T_0}p_2dt-(\rho T_0)^{-1}\int_0^{T_0}p_1dt+\tfrac{1}{2}T_0^{-1}\int_0^{T_0}q_2^2dt$$
$$-\tfrac{1}{2}T_0^{-1}\int_0^{T_0}q_1^2dt+T_0^{-1}\int_0^{T_0}\int_{s_1}^{s_2}\frac{\partial q}{\partial t}ds\,dt=0. \tag{15}$$

The last term on the left hand vanishes since, because of the supposed continuity of the function $q(s,t)$, we can exchange the order of integration and know that q is periodic in t, so that $q(0)=q(T_0)$. Thus for time-average values we can write

$$\overline{p_2}+\tfrac{1}{2}\rho\overline{q_2^2}=\overline{p_1}+\tfrac{1}{2}\rho\overline{q_1^2}. \tag{16}$$

When this equation is applied to our case (figure 4), it follows that

$$p_0+\tfrac{1}{2}\rho U_0^2=\overline{p'}+\tfrac{1}{2}\rho\overline{u'^2}, \tag{17a}$$

$$\overline{p''}+\tfrac{1}{2}\rho\overline{u''^2}=p_0+\tfrac{1}{2}\rho\overline{(U_0+U)^2}. \tag{17b}$$

Taking into account that $u'=u''$, we obtain from equations (17a) and (17b)

$$\overline{\Delta p}=\overline{p''}-\overline{p'}=\tfrac{1}{2}\rho[\overline{(U_0+U(t))^2}-U_0^2]. \tag{18}$$

Therefore, the average thrust $\overline{T}$ is given by

$$\overline{T}=\overline{\Delta p}\,A=\rho U_0 A\,\overline{U(t)}+\tfrac{1}{2}\rho A\,\overline{U^2(t)}. \tag{19}$$

Again this formula yields for the steady case the well-known equation

$$T=\rho A\,U(U_0+\tfrac{1}{2}U). \tag{20}$$

We wish to introduce into equation (19) the perturbation velocity $U_*(t)$ of the fluid particles on the x-axis passing the surface (A) of the jet propeller, the surface where the pressure jump is generated. First, let us recall Euler's equations of incompressible flow

$$\rho\left(\frac{\partial\mathbf{v}}{\partial t}-\mathbf{v}\times\operatorname{curl}\mathbf{v}\right)+\operatorname{grad}\left(\rho\frac{\mathbf{v}^2}{2}+p\right)=\mathbf{F}. \tag{21}$$

Setting

$$\mathbf{v}=U_0\mathbf{i}+\mathbf{v}^*,\quad v^*=\{u^*,v,w\}, \tag{22}$$

assuming that the external forces $\mathbf{F}$ are derivable from a potential V,

$$\mathbf{F}=-\operatorname{grad}V, \tag{23}$$

and neglecting in a first approximation the term $\mathbf{v}^* \times \operatorname{curl} \mathbf{v}^*$ (which certainly is not true for the flow in the wake) we can write

$$\frac{\partial \mathbf{v}^*}{\partial t} + U_0 \frac{\partial \mathbf{v}^*}{\partial x} = -\frac{1}{\rho} \operatorname{grad} H, \tag{24}$$

with

$$H = p + V + \tfrac{1}{2}\rho \mathbf{v}^{*2}. \tag{25}$$

In order to solve equation (24) let

$$\mathbf{v}^* = \operatorname{grad} \phi, \tag{26}$$

where

$$\phi = U(t) \iint_{(A)} \frac{dS}{4\pi R} \tag{27}$$

can be interpreted as the velocity potential of a sink flow of strength $dQ = U(t)\, dS$ at the location of the pressure jump. In the last equation R denotes the distance between an arbitrary point in space P outside (A) and a variable point P' in the surface (A). Substituting equation (26) into equation (24), applying the operation div and recalling the continuity equation

$$\nabla . \mathbf{v} = \nabla . \nabla \phi_0 + \nabla . \nabla \phi = \nabla . \nabla \phi = 0,$$

with $\phi_0 = U_0 x$ as the velocity potential of the translatory flow, we find that H is a potential function, satisfying $\Delta H = 0$. From equations (24) and (26) it follows further that

$$-\frac{4\pi}{\rho} H = 4\pi \left(\frac{\partial \phi}{\partial t} + U_0 \frac{\partial \phi}{\partial x} \right) = \frac{dU(t)}{dt} \iint_{(A)} \frac{dS}{R} + U_0 U(t) \iint_{(A)} \frac{\partial}{\partial x} \left(\frac{1}{R} \right) dS.$$

The surface (A) of the jet propeller where the pressure jump occurs (cross-section a–a) is assumed to be a circular disk of radius R_0 which is perpendicular to the x-axis and whose centre is the origin of our co-ordinate system. If we denote the cylindrical co-ordinates of an arbitrary point P in space by x, r, ψ and those of a variable point P' on the disk by 0, r', ψ', we obtain

$$dS = r'\, dr'\, d\psi'$$

and

$$R = [r'^2 + r^2 + x^2 - 2r'r \cos(\psi' - \psi)]^{\frac{1}{2}}.$$

The velocity u^* along the x-axis ($r = 0$) follows from

$$u^* = \frac{\partial \phi}{\partial x} = \frac{U(t)}{4\pi} \frac{\partial}{\partial x} \int_0^{R_0} \int_0^{2\pi} \frac{r'\, dr'\, d\psi'}{[r'^2 + r^2 + x^2 - 2r'r \cos(\psi' - \psi)]^{\frac{1}{2}}}$$

to yield

$$u^*|_{r=0} = \left. \frac{\partial \phi}{\partial x} \right|_{r=0} = -\frac{U(t)}{4\pi} \int_0^{R_0} \int_0^{2\pi} \frac{x r'\, dr'\, d\psi'}{(r'^2 + x^2)^{\frac{3}{2}}}$$

$$= \frac{U(t)}{2} \left[\frac{x}{(R_0^2 + x^2)^{\frac{1}{2}}} - 1 \right].$$

In order to find the correct value for the wake, we have to add a parallel flow $U(t)$. Hence

$$u^*|_{r=0,\, x>0} = \frac{U(t)}{2} \left[\frac{x}{(R_0^2 + x^2)^{\frac{1}{2}}} + 1 \right].$$

For $x = 0$ we find that

$$u^*|_{r=0,\,x=0} = U_*(t) = \tfrac{1}{2}U(t). \tag{28}$$

Substituting this value for $U(t)$ into equation (19), we have finally

$$\bar{T} = 2\rho A[U_0\overline{U_*(t)} + \overline{U_*^2(t)}]. \tag{29}$$

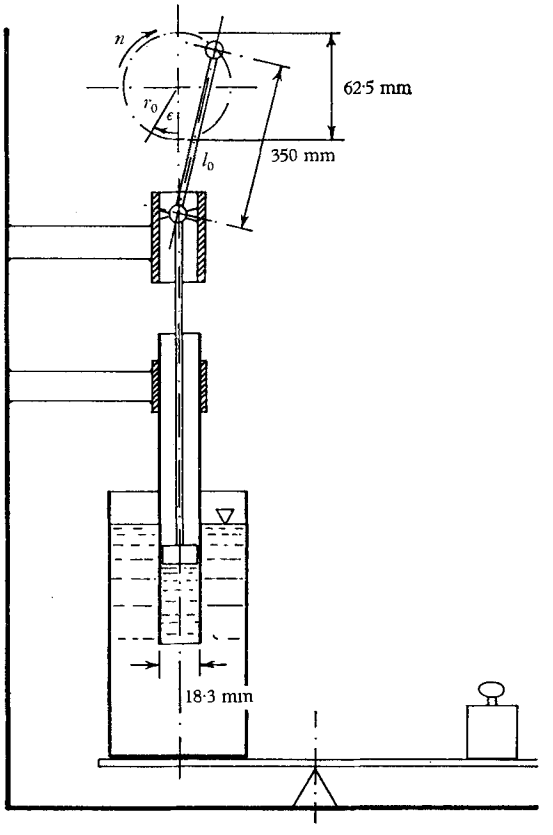

FIGURE 5. Sketch of the test apparatus (proposed by E. G. Finke, Karlsruhe, Germany).

As far as the coefficient of contraction C_0 of the jet is concerned, we remark that in the wake the velocity of the jet is approximately constant across the x-axis. Thus, from the continuity equation for the jet,

$$A[U_0 + U_*(t)] = A_\infty(t)\,[U_0 + U(t)], \tag{30}$$

there follows the relation

$$C_0(t) = \frac{A_\infty(t)}{A} = \frac{U_0 + U_*(t)}{U_0 + U(t)} = \frac{1 + \frac{1}{2}\theta}{1 + \theta} \tag{31}$$

with $\theta = U(t)/U_0$.

Equation (29) can be compared with experimental data obtained by K. Trunz at the Institut für Strömungslehre und Strömungsmaschinen of the Technische Hochschule Karlsruhe, Germany (Dickmann 1950). A schematic sketch of the test apparatus is shown in figure 5. A piston, attached to a drive shaft which is

actuated by a crank, moves sinusoidally up and down in a vertical glass tube, which again is inserted into a large vessel. Then the average thrust value is measured by the reaction on the large container, placed on a highly sensitive balance. The results are plotted in figure 6.

We assume the average velocity of the water at the opening of the cylindrical glass tube to be equal to the velocity of the piston, which is given by

$$c = r_0\omega(\sin\epsilon + \tfrac{1}{2}\lambda\sin 2\epsilon), \tag{32}$$

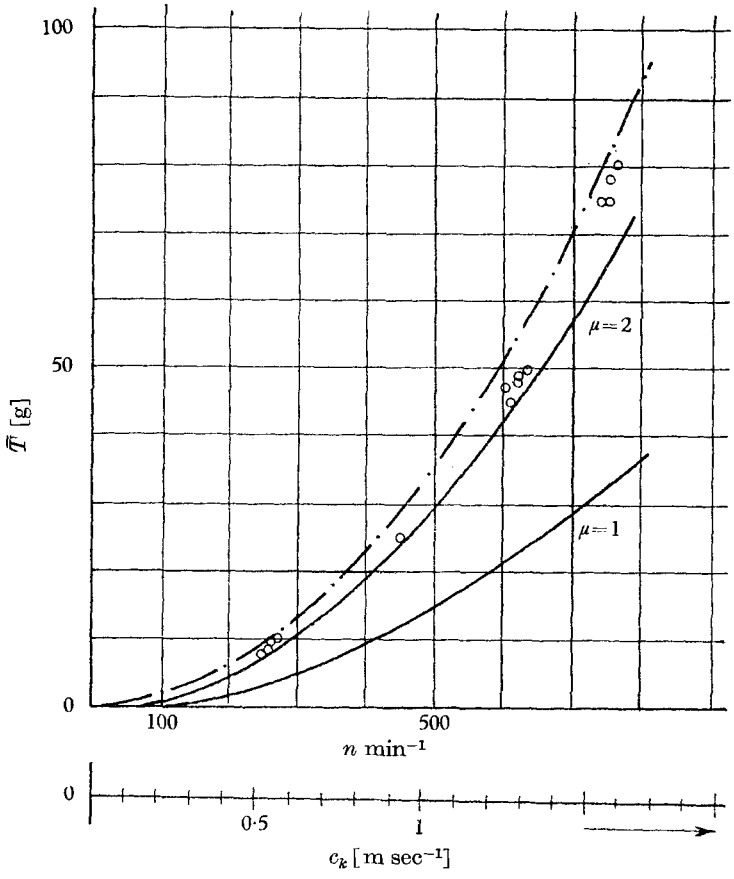

FIGURE 6. Plot of the experimental and theoretical results for the average thrust. The circles represent the experimental values.

where $\epsilon = \omega t$ and $\lambda = r_0/l_0$. The meaning of the symbols used is evident from figure 4. The relation between the angular velocity ω of the crank and the speed of rotation n is given by $\omega^2 = (n\pi/30)^2$. If we say that $U_* = c$, it follows from equation (32) that

$$U_* = r_0\omega\sin\omega t + \tfrac{1}{2}\lambda r_0\omega\sin 2\omega t. \tag{33}$$

In order to apply equation (29) to the present case we set $U_0 = 0$ and obtain

$$\bar{T} = 2\rho A\overline{U_*^2(t)}. \tag{34}$$

Now equation (33) yields the velocity distribution for the full propulsion cycle, i.e.

for the suction and ejection interval. But according to Dickmann (1955) thrust is generated during the ejection interval only; thus we find

$$\overline{U_*^2(t)} = \tfrac{1}{4}(r_0^2\omega^2 + \tfrac{1}{4}\lambda^2 r_0^2\omega^2) \tag{35}$$

and, hence, for the average thrust

$$\overline{T} = \tfrac{1}{2}\rho A r_0^2\omega^2(1 + \tfrac{1}{4}\lambda^2). \tag{36}$$

With the values $\rho = 102\,\mathrm{kg\,sec^2\,m^{-4}}$, $A = 2{\cdot}63 \times 10^{-4}\,\mathrm{m^2}$, $r_0^2 = 9{\cdot}78 \times 10^{-4}\,\mathrm{m^2}$, $\omega^2 = 110 \times (n/100)^2\,\mathrm{sec^{-2}}$, $\frac{1}{4}\lambda^2 = 0{\cdot}002$, the last equation yields

$$\overline{T} = 1{\cdot}435\,(n/100)^2\,[\mathrm{g}]. \tag{37}$$

This function is plotted in figure 6 as a dot-dash line. A comparison with the experimental data shows that these results are smaller than those predicted by theory. However, the agreement is quite satisfactory when the approximations which were made in this analysis are taken into account.

In his paper Dickmann (1950) derives for the average thrust of the jet propeller at rest the formula

$$\overline{T} = \mu\tfrac{1}{2}\rho A c_k^2, \tag{38}$$

where c_k denotes the average velocity of the piston. A factor μ, to be determined by experiments, is introduced in order to fit the experimental results. In figure 6 curves with $\mu = 1$ and $\mu = 2$ are plotted as solid lines; we note that the curve with $\mu = 2$ shows a rather good agreement with the values obtained by measurement.

To determine an approximate value for μ we equate equations (38) and (36), neglecting the term $\frac{1}{4}\lambda^2$ in the latter. Hence

$$\mu = r_0^2\omega^2/c_k^2. \tag{39}$$

Inserting $c_k = 2r_0\omega/\pi$ into the foregoing equation yields

$$\mu = \tfrac{1}{4}\pi^2 = 2{\cdot}47. \tag{40}$$

B. *The two-dimensional theory of the unsteady periodically working jet propeller*

In order to obtain a more realistic model of the mechanism of propulsion we want to dispense with the restriction of a one-dimensional flow pattern and to deal now with a two-dimensional fluid motion. This procedure allows us to treat the wake of the jet propeller as a vortex street with a symmetrical grouping of vortices. This approach can be considered to some extent as an extension of von Kármán's ideas. It should be pointed out of course that the assumed concentration of vortices at singular points is an idealization; however, this prototype of a vortex configuration is not only a special case allowing a simple treatment, but approximates also the state of a vortex distribution with continuous structure after some time. We know from experience that such a structure has a tendency to instability and breaks up into single vortex lumps.

A sketch of the two-dimensional flow behind a jet propeller is shown in figure 7. At the sharp trailing edges of the walls W_1 and W_2 two vortices of equal strength and opposite direction of rotation separate and are carried away to the right. Together with the vortex pairs generated earlier they form a trail of point vortices

in a symmetrical arrangement, so that the eddies of the one row are situated exactly opposite to those of the other row. Photographic pictures showing the beginning of a symmetric vortex street behind a jet propeller are found in the paper by Dickmann (1950). Although such a configuration will change very soon into a formation where the two vortex rows are symmetrically staggered, we suppose a stable geometric pattern of two infinitely extended vortex rows symmetrically spaced. According to Dickmann (1950) the mutual arrangement of vortices is irrelevant regarding the calculation of thrust from a periodic vortex system passing a control surface.

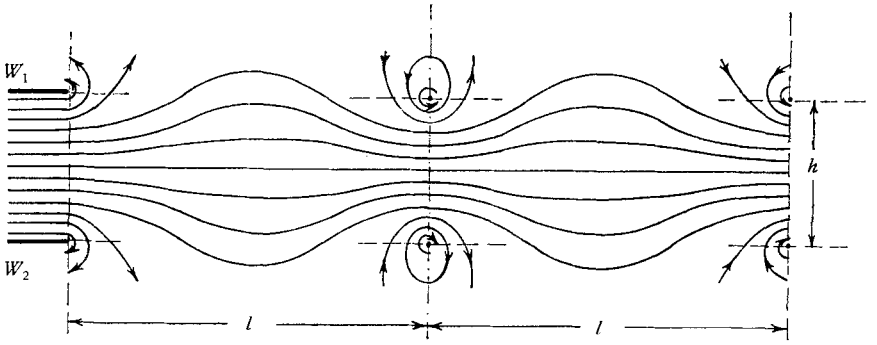

FIGURE 7. Symmetric vortex trail behind a jet propeller.

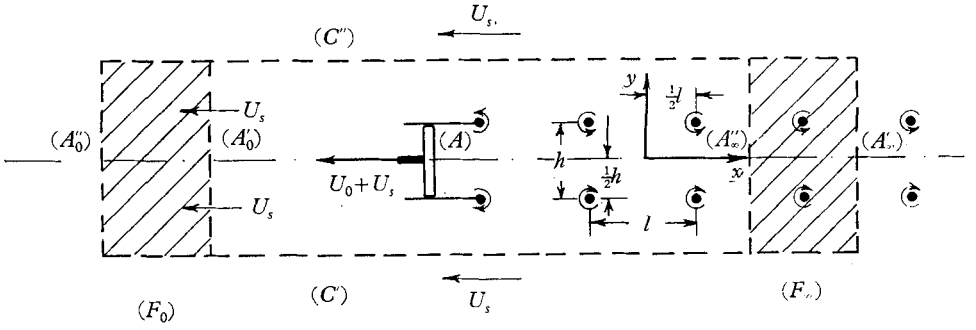

FIGURE 8. Disposition of the control surface.

Figure 8 shows the disposition of the control surface S. The surface (A'_∞) is located so that it intersects the axis of the street perpendicularly between two consecutive vortex pairs. The position of (A'_∞) is far behind the generation of the propulsion; thus, in this region we have only the flow caused by the vortex trail. In the same way we put the surface (A'_0) in front of the jet propeller so that an undisturbed parallel flow may be assumed. Finally, we suppose the control planes (C') and (C'') to be located so far away from the vortex configuration that again an undisturbed parallel flow may be assumed. In the following we shall move the latter surfaces to infinity.

Now let us consider a Cartesian co-ordinate system x, y whose positive x-axis is directed opposite to the direction of motion of the jet propeller. This reference frame is supposed to move with the vortex trail; therefore, in this system the

position of the vortices remains unchanged. The time T_0 the propeller needs to cover a distance l to the left is given by

$$T_0 = l/(U_0 + U_s), \tag{41}$$

where U_0 denotes the constant velocity of the jet propeller and U_s designates the uniform velocity with which the vortex system would move opposite to the direction of motion of the jet propeller in fluid at rest.

During this time interval a pair of vortices is generated at the trailing edge. The flow field in our reference frame is a periodic one but spatially shifted. The two flow patterns in the domain bounded by the control surface are identical at times t and $t+T_0$ except for the newly generated vortex pair. A displacement about l at the instant $t+T_0$ would shift the surfaces (A'_∞) and (A'_0) into positions indicated by (A''_∞) and (A''_0). The advantage of this co-ordinate system is evident.

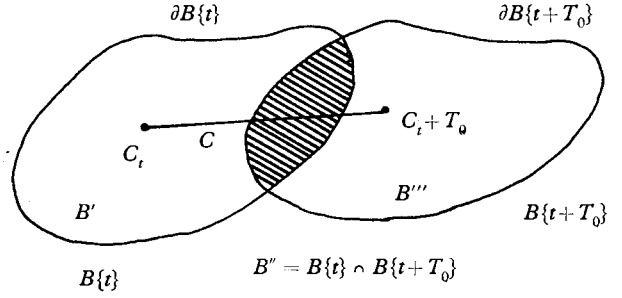

FIGURE 9. Position of the control volume B at instants t and $t+T_0$.

Let us apply now the momentum theorem for an unsteady spatially shifted periodic flow field (figure 9). According to Schiele (1961) we obtain for the three-dimensional flow field the equation

$$\iiint_{B'''} \mathbf{v}(t+T_0)\,d\tau + \iiint_{B'} \mathbf{v}(t+T_0)\,d\tau + \int_t^{t+T_0} \iint_{\partial B} \mathbf{v}(\mathbf{v}\cdot\mathbf{n})\,dS\,dt = -\rho^{-1} \int_t^{t+T_0} \iint_{\partial B} p\mathbf{n}\,dS\,dt \tag{42}$$

where ∂B denotes the boundary of the domain B. Thus, specializing this result to our case, we find that the momentum theorem for the x-component yields

$$\iint_{(F_\infty)} u\,dS - \iint_{(F_0)} u\,dS + \int_t^{t+T_0} \int_{\partial S} u(u\cos\alpha + v\cos\beta)\,ds\,dt + \rho^{-1} \int_t^{t+T_0} \int_{\partial S} \cos\alpha\,ds\,dt = 0, \tag{43}$$

where (F_∞) and (F_0) refer to the shaded regions in figure 8 and ∂S indicates that the integral in question has to be taken along the boundary line of the control surface, that is, along the lines in which the plane surfaces (A), (A'_∞), (A'_0), (C'), (C''), intersect the (x, y)-plane. In order to calculate the terms of equation (43) we determine the velocity components u and v by using the complex potential χ of the flow field which is given by

$$\chi = \chi_1 + \chi_2 = -U_s z + \frac{\Gamma}{2\pi i} \log \frac{\sin \pi(z-z_0)/l}{\sin \pi(z+z_0)/l}, \tag{44}$$

where $z = x + iy$, $i^2 = -1$, χ_1 designates the complex potential of the parallel flow in front and at the side of the control surface and χ_2 refers to the complex potential of the vortex street with point vortices of strength Γ, where the basic vortices of the row are located at $\pm z_0 (z_0 = \frac{1}{2}l + \frac{1}{2}ih)$. We should note that the direction of rotation of the vortices of this trail is opposite to the sense of the Kármán vortices. Differentiation of equation (44) yields the complex velocity

$$W = \frac{d\chi}{dz} = u - iv = -U_s - \frac{\Gamma}{l} \frac{\sinh \pi h/l}{\cosh \pi h/l + \cos 2\pi z/l}. \tag{45}$$

From elementary but protracted calculations for the evaluation of the integrals in equation (43) it follows finally that

$$\overline{T} = \frac{\rho \Gamma h}{T_0} + U_s \frac{\rho \Gamma h}{l} - \frac{1}{2\pi} \frac{\rho \Gamma^2}{l}, \tag{46}$$

where $\overline{T}$ is defined by

$$\overline{T} = -T_0^{-1} \int_t^{t+T_0} \int_{(A)} p \cos \alpha \, dy \, dt, \tag{47}$$

and

$$U_s = (\Gamma/2l) \coth \pi h/l. \tag{48}$$

We remark that in equation (47) the average thrust has a negative sign since we consider the forces exerted upon the liquid.

Inserting the term for T_0 from equation (41) into the thrust formula (46) we obtain

$$\overline{T} = \rho h \frac{\Gamma}{l} \left[U_0 + 2U_s - \frac{1}{2\pi} \frac{\Gamma}{h} \right]. \tag{49}$$

An analysis for the steady case yields

$$T = \lim_{l \to 0,\, \Gamma/l \to \gamma_0} \overline{T} = \rho A_\infty U (U_0 + U) \tag{50}$$

with

$$\gamma_0 = \lim_{l \to 0} \Gamma/l, \tag{51}$$

where γ_0 denotes the finite continuous distribution of the vortex strength of the two plane vortex sheets which form the contour of the jet stream and $A_\infty = h$ denotes the area of reference of the jet stream passing the surface (A'_∞).

Now let us re-write equation (46) by introducing an appropriate Strouhal number. First of all we express in this equation the period T_0 by the frequency $\nu = 1/T_0$; hence

$$\overline{T} = \tfrac{1}{2} \rho h \left[2\nu\Gamma + \frac{\Gamma^2}{l^2} \coth \frac{\pi h}{l} - \frac{1}{\pi} \frac{\Gamma^2}{lh} \right]. \tag{52}$$

With the dimensionless quantities

$$\eta = \overline{T} / \tfrac{1}{2} \rho h U_0^2, \tag{53}$$

where the average thrust has been related to A_∞, and

$$\kappa = \Gamma / l U_0, \tag{54}$$

we find

$$\eta = \kappa^2 \left[2 \frac{\nu l}{\Gamma/l} + \coth \frac{\pi h}{l} - \frac{l}{\pi h} \right]. \tag{55}$$

Defining now a Strouhal number σ by

$$\sigma = \nu l/(\Gamma/l), \tag{56}$$

and putting

$$\zeta' = \coth\frac{\pi h}{l} - \frac{l}{\pi h}, \tag{57}$$

we obtain finally

$$\eta = \kappa^2(2\sigma + \zeta'). \tag{58}$$

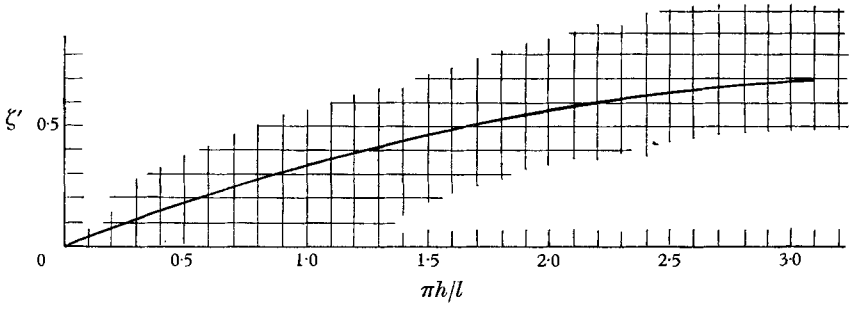

FIGURE 10. Plot of function ζ' *vs* $\pi h/l$.

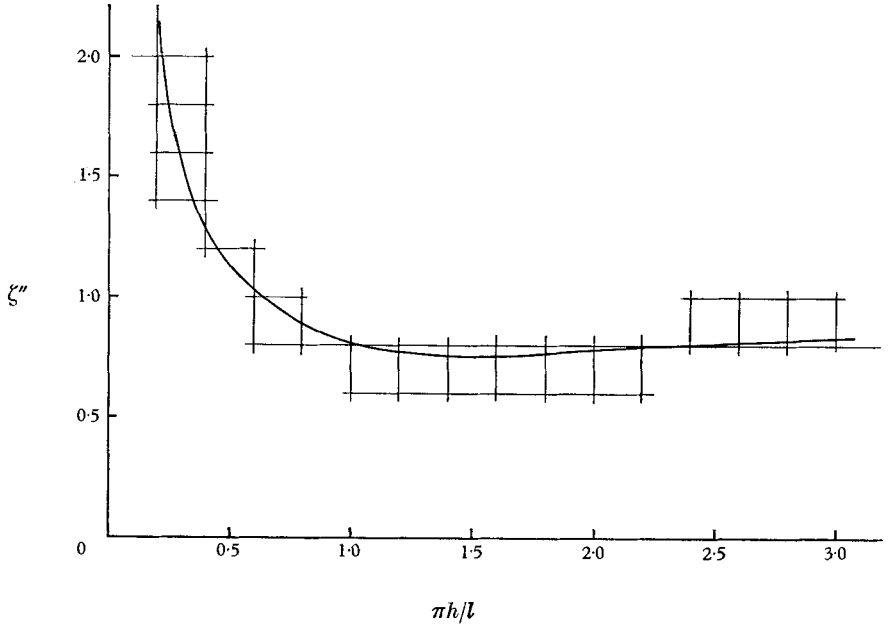

FIGURE 11. Plot of function ζ'' *vs* $\pi h/l$.

A plot of the function ζ', which depends on the geometry of the vortex trail only, is given in figure (10). It should be pointed out that equation (58) might be especially suitable to represent experimental results.

Elimination of the Strouhal number from the last equation yields

$$\eta = 2\kappa(1 + \kappa\zeta''), \tag{59}$$

where

$$\zeta'' = \coth(\pi h/l) - l/2\pi h \tag{60}$$

depends again on the geometric configuration of the vortex street only. A plot of this function is shown in figure 11. The connexion between ζ' and ζ'' is easily found to be $\zeta''-\zeta' = l/2\pi h$. Figures 12 and 13 show plots of η against κ (parameter $\pi h/l$) and $\pi h/l$ (parameter κ).

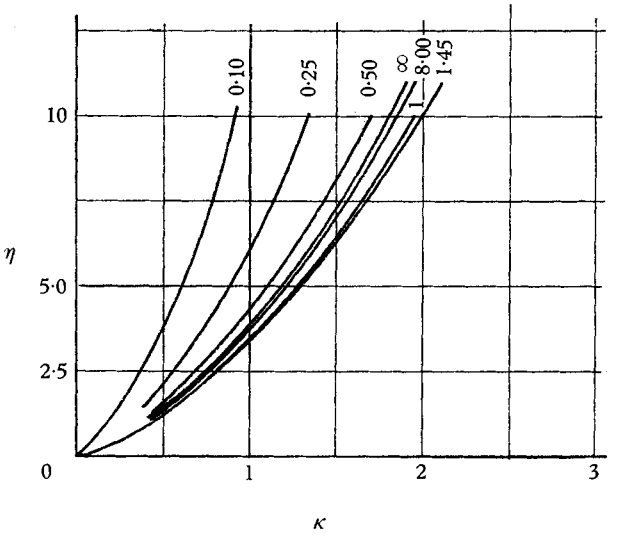

FIGURE 12. Plot of function η *vs* κ. The numbers represent the appropriate values of $\pi h/l$.

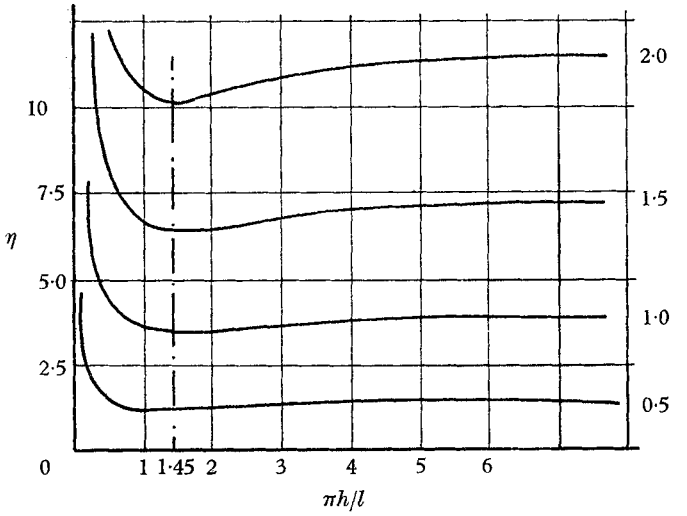

FIGURE 13. Plot of function η *vs* $\pi h/l$. The numbers at the right represent the values of κ.

3. Remarks on the equation of motion

Let us consider the translatory motion of a torpedo-shaped rigid body Σ along a given horizontal axis.

The body travels, prior to the onset of a motion cycle, with a constant initial average speed U_0 in water at rest. It is assumed that thrust is produced only

during the thrust interval; afterwards the submerged body coasts until the next cycle begins. The maximum speed u_1 will occur at the end of the thrust interval and the minimum speed u_2 will occur at the end of the coasting interval. Then Newton's second law yields the equation of motion during acceleration and deceleration

$$M\frac{du}{dt} = T_i - D_i, \tag{61}$$

with $u = u(t)$ as the instantaneous body speed, T_i as the instantaneous thrust, D_i as the instantaneous drag and M as the virtual mass, which is given by

$$M = m' + m'', \tag{62}$$

with m' as (actual) body mass and m'' as 'added' mass. The latter term can be written in the form

$$m'' = k_0 m_0 = k_0 \rho v, \tag{63}$$

where m_0 and v denote the mass and volume of liquid displaced, k_0 a coefficient depending on the shape of the body, and ρ the density of the water. Although we are concerned with the problem of the motion of a body with variable mass, we assume for the sake of simplicity that M is approximately constant.

In order to derive a reasonable approximation for T_i we recall the relation

$$T = \rho A U(U_0 + \tfrac{1}{2}U) \tag{64}$$

holding for steady exhaust, where at present U denotes the absolute velocity of the jet at the discharge nozzle. Between U and U_*, the jet velocity relative to the orifice, there exists the relation

$$U = U_* - U_0. \tag{65}$$

Inserting this into equation (64) and remembering that $U_* = \frac{1}{2}U$, we obtain

$$T = \rho A(U_*^2 - U_0^2). \tag{66}$$

Replacing U_0 by the instantaneous body speed u we have

$$T^* = \rho A(U_*^2 - u^2). \tag{67}$$

We now make the assumption that we can substitute $\bar{T}$, the average thrust produced during a full propulsion cycle with period T_0, for T^*. The time period τ of a full motion cycle consists of a thrust and a coast interval of duration τ' and τ'', respectively. Thus

$$\tau = \tau' + \tau'', \tag{68}$$

with
$$\tau = NT_0, \quad \tau' = N'T_0, \quad \tau'' = N''T_0; \quad N = N' + N'', \tag{69}$$

where N, N', and N'' designate the number of pulses occurring during a full motion cycle, the thrust interval and the coast interval, respectively. This yields for T_i approximately

$$T_i = N'T^* = N'\rho A(U_*^2 - u^2), \tag{70}$$

or with
$$K' = N'\rho A, \tag{71}$$

finally
$$T_i = K'(U_*^2 - u^2). \tag{72}$$

The instantaneous drag D_i can be conveniently expressed by

$$D_i = \tfrac{1}{2}c_0 V_0^{\frac{2}{3}} \rho u^2 \tag{73}$$

with c_0 as an experimental coefficient depending on the shape of the body and V_0 as the submerged body volume, which in our case is equal to the volume of the body itself. Putting

$$K'' = \tfrac{1}{2} c_0 V_0^{\frac{2}{3}} \rho, \tag{74}$$

we obtain

$$D_i = K'' u^2. \tag{75}$$

Hence we have the following differential equation of motion for the acceleration period (thrust interval)

$$M \frac{du}{dt} = K' U_*^2 - (K' + K'') u^2. \tag{76}$$

Setting

$$\frac{K'}{M} U_*^2 = C_1, \quad \frac{K' + K''}{M} = C_2, \tag{77}$$

it follows from equations (76) and (77) that

$$\frac{du}{dt} = C_1 - C_2 u^2. \tag{78}$$

Integration of this simple Riccati equation yields

$$t + \tau_0 = \frac{1}{2K} \log \frac{K + C_2 u}{K - C_2 u}, \tag{79}$$

or

$$u = \frac{K}{C_2} \tanh K(t + \tau_0), \tag{80}$$

with $K = (C_1 C_2)^{\frac{1}{2}}$ and the integration constant

$$\tau_0 = \frac{1}{2K} \log \frac{K + C_2 U_0}{K - C_2 U_0}, \tag{81}$$

resulting from the initial condition $u(0) = U_0$. The velocity u_1 at the end of the thrust interval follows from $u_1 = u(\tau')$. The distance s_1 covered during this time is given by

$$s_1 = \int_0^{\tau'} u(t)\, dt = \frac{1}{C_2} \log \frac{\cosh K(\tau' + \tau_0)}{\cosh K \tau_0}. \tag{82}$$

The coast period is described by the equation

$$M \frac{du}{dt} = -D_i \tag{83}$$

or

$$\frac{du}{dt} = -\frac{K''}{M} u^2. \tag{84}$$

Integration yields

$$u = \left\{ \frac{K''}{M} t + k \right\}^{-1}, \tag{85}$$

where the integration constant

$$k = \frac{1}{u_1} - \frac{K'}{M} \tau' \tag{86}$$

is determined by the initial condition $u(\tau') = u_1$. During the coast interval the velocity of the body decreases and attains, at the end of the motion cycle ($t = \tau$), the value

$$u_2 = \frac{u_1}{1 + (K''/M) \tau'' u_1}. \tag{87}$$

For the distance s_2 covered during the duration of the coast interval, we find

$$s_2 = \int_{\tau'}^{\tau} u(t)\,dt = \frac{M}{K''}\log\left(\frac{K''}{M}u_1\tau'' + 1\right). \tag{88}$$

The results derived so far are based on the integration theory of the differential equation of motion under the hypothesis that the instantaneous thrust can be approximated with sufficient accuracy by equation (70). Another approach relating the average thrust, produced during the thrust interval, somewhat more to observation relies on the momentum principle. Neglecting drag we obtain

$$\int_0^{\tau'} T(t)dt = M(u_1 - U_0). \tag{89}$$

Therefore with

$$\int_0^{\tau'} T(t)dt = T(t_0)\tau' \approx T_i\tau' \quad (0 < t_0 < \tau'), \tag{90}$$

we can write

$$T_i \approx M\frac{u_1 - U_0}{\tau'} = K_0 = \text{const.} \tag{91}$$

Hence, for the acceleration period

$$M\frac{du}{dt} = K_0 - K''u^2. \tag{92}$$

Putting

$$\frac{K_0}{M} = C_1^*, \quad \frac{K''}{M} = C_2^*, \tag{93}$$

we obtain a differential equation having the same structure as the foregoing equation (78) except the meaning of the constants. For the deceleration period (coast interval) equation (83) holds again.

It would be desirable to apply the theoretical results of this analysis to the actual motion of a squid or octopus and to compare calculated data with those obtained by observation. However, very little authentic information is available regarding the swimming speed of squids. According to the American marine zoologist, Conrad Limbaugh, the common Pacific squid (Loligo opalescens) 'travels approximately 5–8 m.p.h. judging from those being chased by sea lions. Common heavy-bodied squids in the Bahamas travel approximately 4–6 m.p.h.' (Lane 1960, p. 60). A report by Commander Arne Groenningsaeter of the Royal Norwegian Navy (Lane 1960, p. 223) indicates swimming speeds of large squids in the region of some 20 m.p.h., which seems reasonable for a large ommastrephid.

Concerning octopuses we want to remark that they are generally not such fast swimmers as squids and cuttlefish. Joseph Sinel, whose studies are based chiefly on the common octopus (*Octopus vulgaris*) in the Channel Islands, gives the speed of one with a two-foot span as about 8 m.p.h. Each expelled jet drives the octopus 6–8 ft. The distance is much greater in squids of comparable size, owing to their more powerful jets and streamlined shape (Lane 1960, p. 68).

These few statements point out clearly that a close agreement between data calculated from observations and theoretical results predicted by the present analysis is not to be expected. Much work remains to be done with regard to

observation as well as improvements of the approach of this study in order to relate in a more realistic way the functioning of a model to the actual situation in a squid.

REFERENCES

DICKMANN, H. E. 1950 Schiffsantrieb mit instationären Vortriebsorganen. *Schiff und Hafen*, Heft 10.

HALEY, A. G. 1958 *Rocketry and Space Exploration*, p. 2. New York: D. Van Nostrand Co.

LANE, F. W. 1960 *Kingdom of the Octopus. The Life History of the Cephalopodia*. New York: Sheridan House.

PRANDTL, L. 1952. *Essentials of Fluid Dynamics*. New York: Hafner Publishing Co.

SCHIELE, O. 1961 *Ein Beitrag zur Theorie instationär und periodisch arbeitender Propulsionsorgane*. Dissertation Technische Hochschule Karlsruhe (Germany).